VI International Conference on Computational Methods for Coupled Problems in Science and Engineering
COUPLED PROBLEMS 2015
B. Schrefler, E. Oñate and M. Papadrakakis (Eds)

MULTIPHYSICS FINITE – ELEMENT MODELLING OF AN ALL – VANADIUM REDOX FLOW BATTERY FOR STATIONARY ENERGY STORAGE

F. MORO, A. BERTUCCO, V. FIORENZATO, M. GIOMO, AND M. GUARNIERI

Dipartimento di Ingegneria Industriale (DII)
Università degli Studi di Padova
Via Gradenigo 6/A, 35131 Padova, Italy
e-mail: federico.moro@unipd.it

Key words: Coupled Problems, Multiphysics Problems, Redox Flow Battery, Vanadium, Energy Storage.

This work was supported by the University of Padova under the MAESTRA 2011 strategic project.

Abstract. All-Vanadium Redox Flow Batteries (VRFBs) are emerging as a novel technology for stationary energy storage. Numerical models are useful for exploring the potential performance of such devices, optimizing the structure and operating condition of cell stacks, and studying its interfacing to the electrical grid. A one-dimensional steady-state multiphysics model of a single VRFB, including mass, charge and momentum transport and conservation, and coupled to a kinetic model for electrochemical reactions, is first presented. This model is then extended, including reservoir equations, in order to simulate the VRFB charge and discharge dynamics. These multiphysics models are discretized by the finite element method in a commercial software package (COMSOL). Numerical results of both static and dynamic 1D models are compared to those from 2D models, with the same parameters, showing good agreement. This motivates the use of reduced models for a more efficient system simulation.

1 INTRODUCTION

The growing penetration of renewable sources in the electric grid has boosted the development of new technologies for stationary energy storage. All-Vanadium Redox Flow Batteries exhibit a very high potential for both medium and large scale applications. This is due to power/energy independent sizing, high round-trip efficiency, room temperature operation, and long charge/discharge cycle life. A number of challenges need to be tackled in order to gain full commercial success, regarding single cell and stack design, highly efficient energy-conversion materials, and optimal power management and control operations [1].

Numerical models are powerful tools in designing control and monitoring systems, which are needed for interfacing the stack to the electric grid. Both 1D and 2D finite element models have been developed in order to reduce computing cost in comparison with 3D models and allow for a real-time simulation of VRFB operations. A considerably complete and

comprehensive 2D distributed model, able of capturing time variations of current density and species concentrations inside the cell, was first developed by Shah et al. [2]. Vanadium crossover and related losses were accounted for in [3]. A 2D steady-state model, showing good agreement with experiments despite its simplicity, was later proposed by You et al. [4]. To simulate a VRFB stack rather than a single cell, Vynnycky proposed an asymptotic reduction approach to obtain a 1D multiphysics model for a single electrochemical cell. An enhanced version of this model, with concentration dependent kinetics, was presented in [5].

Starting from this work, a novel 1D steady-state finite-element model of an all-vanadium redox flow battery is here proposed. A typical VRFB cell (Fig.1) consists of: the positive and the negative porous layers where chemical half-reactions occur, the separation polymer membrane for proton conduction, and the current collectors which convey the electrons to/from the external circuit. The FEM model incorporates the following multiphysics equations: momentum, charge and species conservation, mass transport (Nernst-Plank equation), electric conduction, charge generation (Butler-Volmer equation) inside the porous electrodes, and the proton conduction inside the membrane. In particular, the effect of mass transport on the charge generation is taken into account by considering the electrode surface concentrations, which differ from bulk concentrations. Differently from [5], the 1D model is implemented within a commercial software package (COMSOL) and takes into account the behaviour of the current collectors in order to achieve a more accurate representation of the device. The independent variables of the model are the electrode and electrolyte potentials and the ionic species concentrations in the electrodes. The cell voltage is obtained from the electrode potential as a function of the State of Charge (SoC).

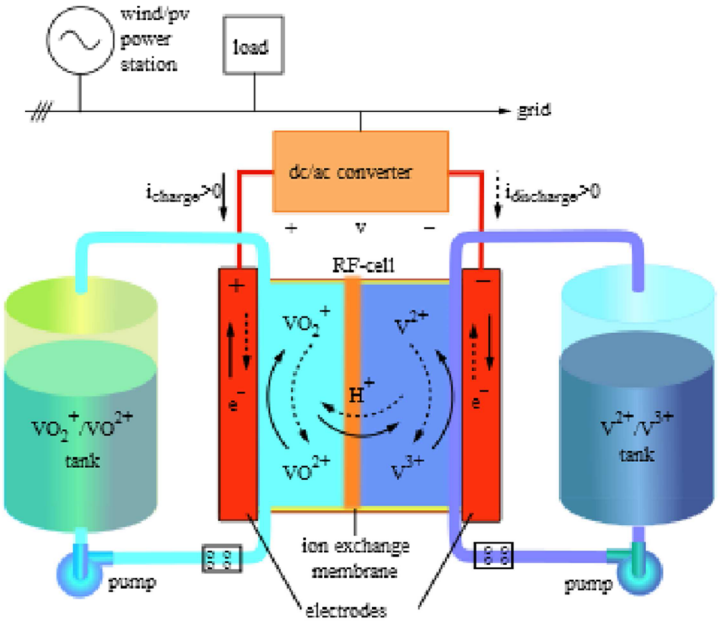

Figure 1: Schematic diagram of a VRFB (collectors + porous electrodes + polymeric membrane) interfaced to the electrical grid by a DC/AC converter. Electrolytes, stored in separated tanks, are pumped to the VRFB.

2 MULTIPHYSICS MODEL

Fig. 1 shows a schematic diagram of a VRFB cell interfaced to the electrical grid. Energy conversion occurring inside VRFBs is based on the following electrochemical reduction and oxidation reactions at the electrode-electrolyte interface:

$$VO^{2+} + H_2O \rightleftarrows VO_2^+ + 2H^+ + e^- \quad \text{(positive half-cell)} \tag{1}$$

$$V^{3+} + e^- \rightleftarrows V^{2+} \quad \text{(negative half-cell)}$$

The electrolytes are vanadium oxides dissolved in a sulphuric acid water solution (1–5 M concentration). Arrows in (1) indicate the charge/discharge operations, e.g. the rightward arrows indicate the charging phase when VO_2^+ and V^{2+} are generated at the positive and negative electrode, respectively. During the charging operation the reduction half-reaction at the negative electrode extracts electrons from the collector and ions from the electrolyte, while the oxidation half-reaction at the other electrode provides electrons to the collector. Protons H^+ migrate from one electrode to the other (from anode to cathode) through a polymer electrolyte (membrane) that is impermeable to electrons, which are thus forced through the external circuit producing an electrical energy exchange.

2.1 Porous electrode equations

The electric charge is generated or consumed at the electrolyte-solid phase interfaces by chemical half-reactions. The reaction kinetics are modeled by using general expressions, derived from the classical Bulter-Volmer equation, which does not take into account the difference between surface and bulk concentrations. Following [5], charge generation rates at positive (1) and negative (2) electrodes are:

$$\begin{aligned} J_{g1} &= J_1^0 \left[\frac{c_{V4,s}}{c_{V4}} \exp\left(\frac{\alpha_{1a} F}{R\,T}\eta_1\right) - \frac{c_{V5,s}}{c_{V5}} \exp\left(-\frac{\alpha_{1c} F}{R\,T}\eta_1\right) \right] \\ J_{g2} &= J_2^0 \left[\frac{c_{V2,s}}{c_{V2}} \exp\left(\frac{\alpha_{2a} F}{R\,T}\eta_2\right) - \frac{c_{V3,s}}{c_{V3}} \exp\left(-\frac{\alpha_{2c} F}{R\,T}\eta_2\right) \right] \end{aligned} \tag{1}$$

where J_1^0, J_2^0 are (concentration dependent) exchange current densities, $c_{i,s}$ are electrolyte surface concentrations at the interface (which generally differ from bulk ones, c_i), $\alpha_{1,a}, \alpha_{2,a}$ and $\alpha_{1,c}, \alpha_{2,c}$ are the anodic and cathodic charge transfer coefficients, and R, T, F are constants (ideal gas and Faraday constants and temperature). Overpotentials in (1) are:

$$\begin{aligned} \eta_1 &= \phi_s - \phi_e - E_1 \\ \eta_2 &= \phi_s - \phi_e - E_2 \end{aligned} \tag{2}$$

where ϕ_s, ϕ_e are the electric potential in the solid phase and the electrolyte. The open circuit voltage (OCV) of each half-cell is calculated according to the Nernst equation as follows:

$$\begin{aligned} E_1 &= E_{0,1} + \frac{R\,T}{F} \log\left(\frac{a_{V5} a_{H^+}^2}{a_{V4}}\right) \\ E_2 &= E_{0,2} + \frac{R\,T}{F} \log\left(\frac{a_{V3}}{a_{V2}}\right) \end{aligned} \tag{3}$$

where $E_{0,1}, E_{0,2}$ are the equilibrium cell potentials in standard conditions.

The electrochemical energy conversion occurs inside porous electrodes, where reactants and products are delivered. Ion species migration in porous electrodes is governed with a mass concentration equation, which is steady-state conditions becomes:

$$\nabla \cdot \boldsymbol{N}_i = S_i \tag{4}$$

where $\boldsymbol{N}_i$ is the molar flux of the i^{th} ion species in the porous medium and S_i is the source term of electrochemical half-reactions. For the positive electrode $i \in \{V_4, V_5, H_1^+, SO_4^-\}$ and for the negative electrode $i \in \{V_2, V_3, H_2^+, SO_4^-\}$. Source terms for these species are: $S_{V4} = -A\,J_{g1}/F$, $S_{V5} = A\,J_{g1}/F$, $S_{H_1^+} = 2A\,J_{g1}/F$, $S_{V2} = -A\,J_{g2}/F$, $S_{V3} = A\,J_{g2}/F$, $S_{H_2^+} = 0$.

The flow density is then composed of three source terms: molecular diffusion, migration due to electric field, and advection. By assuming dilute electrolyte concentrations, this can be modeled by using the Nernst-Plank equation:

$$\boldsymbol{N}_i = -D_i^{eff} \nabla\, c_i - \frac{z_i c_i}{RT} D_i^{eff} F\, \nabla \phi_e + \boldsymbol{v}\, c_i \tag{5}$$

where z_i, c_i are the valence and molar concentration of the i^{th} species, and $\boldsymbol{v}$ is the velocity.

The effective diffusivity is given by Bruggeman correction to molecular diffusivity, i.e. $D_i^{eff} = \epsilon^{3/2} D_i$, where ϵ is the electrode porosity. The electrolyte velocity in porous media is governed by Darcy's law, in which a Kozeny-Carmen law is used for the hydraulic conductivity in the porous felt

$$\boldsymbol{v} = -\frac{d_f^2}{K\,\mu} \frac{\epsilon^3}{1-\epsilon^2} \nabla p \tag{6}$$

where d_f is the porous felt fiber diameter, K is the Kozeny-Carman constant, μ is the dynamic viscosity of the fluid, and p is the pressure. The velocity field can be derived from (6) by using the continuity condition for an incompressible liquid, i.e. $\nabla \cdot \boldsymbol{v} = 0$, and the assumption of dilute solutions. The continuity condition is useful to obtain advection-diffusion equations by combining (4) and (5). Neglecting the electro-migration term produced by the potential gradient, the following equation is obtained:

$$-D_i^{eff} \nabla^2\, c_i + \boldsymbol{v}\, \nabla c_i = S_i \tag{7}$$

which can be simplified, under the 1D assumption proposed in [5], as:

$$-D_i^{eff} \frac{\partial^2 c_i}{\partial x^2} + v_y \frac{c_i - c_i^{in}}{L} = S_i \tag{8}$$

where c_i becomes the average bulk concentrations (depending only on x), $v_y = \frac{Q}{w h_e}$ is the (equivalent) electrolyte velocity along the flow direction y, Q is the volumetric flow rate, w is the electrode width, and h_e is the electrode thickness.

The charge transfer from the electrolyte to the carbon felt occurs at the interface between solid and liquid phases. Charge balance equations are written for an equivalent volume element, considering thus an averaged volumetric current density:

$$\nabla \cdot \boldsymbol{J}_e = -\nabla \cdot \boldsymbol{J}_s = J_{vol} \tag{9}$$

where $\boldsymbol{J_e}$ and $\boldsymbol{J_s}$ are the current density in the electrolyte and in the solid phase, respectively. The volumetric current density is $J_{vol} = -A\,J_{g1}$ (in the positive electrode) or $J_{vol} = A\,J_{g2}$ (in the negative electrode), where A is the specific surface area (m^2/m^3) which denotes the electrochemical active area for unit volume of electrode. The current density inside the electrolyte is only given by the ion migration so that:

$$\boldsymbol{J_e} = \sum_i z_i\,F\,\boldsymbol{N}_i \tag{10}$$

which, by letting expression (5) for the species molar flux, gives:

$$\boldsymbol{J_e} = -K^{eff}\,\nabla\phi_e - F\sum_i z_i\,D_i^{eff}\nabla c_i \tag{11}$$

where $K^{eff} = \frac{F^2}{RT}\sum_i z_i^2\,D_i^{eff}c_i$ is the effective ionic conductivity. In the solid phase, the current density is only given by the electronic conduction, and, by applying the Bruggeman correction on the felt conductivity $\sigma_s^{eff} = (1-\epsilon)^{3/2}\,\sigma_s$, this becomes:

$$\boldsymbol{J_s} = -\sigma_s^{eff}\nabla\phi_s \tag{12}$$

Electrical conduction equations, needed to obtain the electric potential distributions, are finally obtained by letting (11) and (12) in charge balance equations.

The independent variables of the model in the porous electrodes are the electrolyte and the solid phase potential ϕ_e, ϕ_s, and the species concentrations $c_{V2}, c_{V3}, c_{V4}, c_{V5}, c_{H^+}$. The sulphate ion concentration $c_{SO_4^-}$ is finally obtained from the electro-neutrality condition:

$$\sum_i z_i c_i = 0 \tag{13}$$

Homogeneous Neumann boundary conditions are applied for ϕ_e, while homogeneous Dirichlet boundary conditions are applied at the positive electrode for ϕ_s. The current density J_{coll}, which can be positive (charge) or negative (discharge), is applied at the positive electrode. Inlet concentrations for all ionic species are related to the SoC of the electrolyte:

$$\begin{aligned}
c_{H^+,1}^{in} &= c_{H^+,1}^0 + c_{V,1}\,SoC \\
c_{H^+,1}^{in} &= c_{H^+,1}^0 + c_{V,1}\,SoC \\
c_{V_4}^{in} &= c_{V_4}^0 + c_{V,1}(1-SoC) \\
c_{V_5}^{in} &= c_{V_5}^0 + c_{V,2}\,SoC \\
c_{V_2}^{in} &= c_{V_2}^0 + c_{V,2}\,SoC \\
c_{V_3}^{in} &= c_{V_3}^0 + c_{V,2}\,(1-SoC)
\end{aligned} \tag{14}$$

where $SoC = \frac{c_{V5}}{c_{V,1}} = \frac{c_{V2}}{c_{V,2}}$ is the State of Charge ($SoC = 0$ when the redox flow cell is fully charged, $SoC = 1$ when it is fully discharged) and $c_{V,1} = c_{V4} + c_{V5}$, $c_{V,2} = c_{V2} + c_{V3}$ are the total vanadium concentrations at the positive and negative electrodes, respectively.

2.2 Membrane and current collector equations

Electric charges generated and consumed at porous electrodes are drawn by the current collectors according to Ohm's law for electronic conductors, i.e. $\boldsymbol{J_s} = -\sigma_c\,\nabla\phi_s$, where σ_c is

the (uniform) electronic conductivity. This relationship, combined with the charge conservation equation, provides:

$$-\nabla \cdot \sigma_c \, \phi_s = 0 \tag{15}$$

The polymer membrane provides the protonic exchange and only a ionic current occurs in it, so that electrons are forced to the external circuit. The electrical behavior of the membrane, which can be regarded as a solid electrolyte, is characterized by the conduction equation:

$$-\nabla \cdot \sigma_m^{eff} \, \phi_s = 0 \tag{16}$$

where $\sigma_m^{eff} = \frac{z_{H^+}^2 \, F^2 \, c_f \, D_{H^+}}{R \, T}$ is the effective conductivity of the membrane, with z_{H^+} proton valence, c_f concentration of fixed charge sites, and D_{H^+} the proton diffusion coefficient.

2.2 Dynamic model equations

During VRFB operations the species concentrations in the reservoirs vary due to the processes occurring in the half-cells. Having assumed the conservation of volumes [2], the volumetric flow rate at the outlet of the electrodes is $Q = v_y \, w \, L$. The outlet concentrations are calculated by averaging along the outlet surfaces. The changes in species concentrations at the inlet of the electrodes due to recirculation can be calculated from the following material balance, which assumes perfect mixing and negligible reaction in the reservoir of volume V:

$$\frac{dc_i^{in}}{dt} = \frac{Q}{V}\left(c_i^{out} - c_i^{in}\right), \qquad c_i^{in}(0) = c_i^0 \tag{17}$$

The reservoir volume is obtained by subtracting the electrode volume ($\varepsilon \, L w h_e$) from the volume of electrolyte on each side of cell, V_T . The electrolyte volume can be estimated from Faraday law once the electrical current I and the charge time Δt_{ch} have been fixed, as:

$$V = \frac{I \, \Delta t_{ch}}{F\left(c_{V5}^f - c_{V5}^0\right)} \tag{18}$$

where c_{V5}^0 and c_{V5}^f are the initial and the final (estimated) concentrations of VO_2^+. The volume of electrolyte in the pipes and pump is assumed to be negligible. To account for the evolution in species concentration, the conservation equation (7) is modified as follows:

$$\frac{\partial \, \epsilon \, c_i}{\partial \, t} = S_i + D_i^{eff} \nabla^2 \, c_i - \boldsymbol{v} \, \nabla c_i \tag{19}$$

and a similar expression, corresponding to (8), is obtained under the 1D assumption:

$$\frac{\partial \, \epsilon \, c_i}{\partial \, t} = S_i + D_i^{eff} \frac{\partial^2 c_i}{\partial x^2} - v_y \frac{c_i - c_i^{in}}{L} \tag{20}$$

3 NUMERICAL RESULTS

The 1D redox flow battery model is constructed from the previous non-linear equations: momentum, charge and species conservation, mass transport (Nernst-Plank equation), electric conduction, charge generation (Butler-Volmer equation) inside the porous electrodes, and the proton conduction inside the membrane. The basic assumption of the model regards the derivation of equation (8), and consists in approximating the concentration gradient inside the porous electrode with a finite difference. The partial differential equations (PDEs) for the 1D model are then simply expressed by substituting the gradient operator with ∂_x (derivative along the horizontal $x-$axis in Fig. 2) where electrical conduction and species diffusion occur. The numerical model is implemented in COMSOL®, which provides a robust simulation environment for multiphysics problems. This software, based on the finite element method (FEM) for the discretization of 1D, 2D, 3D PDEs, provides different non-linear solvers.

In order to assess the validity and the accuracy of the dimensional reduction numerical results of the 1D model are compared with those of a 2D model based on the same physical parameters. The meaning of the geometrical parameters of the 2D model is reported in the schematic of Fig. 2. The 1D model geometry consists in the union of intervals $[X_i, X_{i+1}]$.

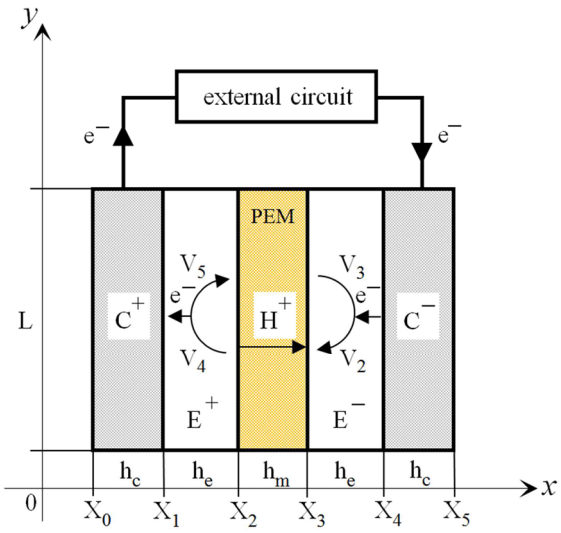

Figure 2: Geometrical parameters in the schematic diagram of 2D VRFB model (C^+, C^-: collectors; E^+, E^-: porous electrodes; PEM: polymer membrane) implemented in COMSOL Multiphysics®.

Due to the generality of PDEs defined in the fully coupled model, "General Form PDE" study nodes were used to implement both conduction and advection-diffusion equations in COMSOL. In particular, (8) was implemented as a diffusion-adsorption equation in order to account for the concentration gradient approximation. The degrees of freedom (DoF) of the discrete algebraic system are concentrations $c_{V4}, c_{V5}, c_{H_1^+}$ (positive electrode) $c_{V2}, c_{V3}, c_{H_2^+}$ (negative electrode), the electrolyte potential ϕ_e (membrane and electrodes), and solid phase potential ϕ_s (electrodes and collectors). These equations, discretized with quadratic finite elements (for both 1D and 2D) defined on structured meshes, were solved by the Newton-Raphson method with a fixed tolerance of 10^{-6}.

The following computing performances were observed in both FEM steady-state models (1D vs. 2D) run on a Intel® Core™@2.70 GHz Processor, 64 bit system, 4 GB RAM: 7.235 vs. 127.361 (number of DoF); 26 s vs. 899 s (solution time); 890 MB vs. 1.89 GB (physical memory); 1.094 MB vs. 2.16 GB (virtual memory). Steady-state solutions of the fully coupled problem were obtained by a parametric sweep (for SoC values ranging from 0.1 to 0.9), after imposing the electric current density J_{coll} at the positive electrode and the inlet species concentrations (14). Geometrical and physical parameters in Tables I and II, used for both 1D and 2D models, were taken from [5] except for the thickness of collectors, which is here presumed. The electrical behavior of the redox flow battery was investigated by computing the electrical cell voltage between the positive and negative current collectors.

Fig. 3 shows that charge and discharge curves of 1D and 2D models are in very good agreement, also with experimental data presented in [5]. The electrolyte and the electrode current density (for the 2D model, in particular, the x-component is considered) in Fig. 4 show a similar behavior. Product and reactant species concentrations at positive and negative electrodes are compared by considering, for the 2D model, the concentration profiles at the electrode outlets ($y = L$). Also in the case of non-electrical variables it can be observed that the reduced model provides high accuracy, even though its complexity is much smaller. The concentration variation inside the device is captured by the 2D model, i.e. Fig. 7 and 8 show that for reactants the concentration is higher near the inlet, whereas for products the concentration is higher near the outlet.

Dynamic 1D and 2D models are constructed by adding the reservoir equation and by enforcing time-varying boundary conditions at the electrode inlets. Time profiles of model variables were obtained by an adaptive time-stepping backward Euler solver. Computing time and memory requirements, with the same computer as above, were 710 s and 1.86 GB for the 2D model, and 232 s and 1.91 GB for the 1D model. Fig. 9 and 10 show that the reduced model again provides an accurate information about multiphysics problem variables.

4 CONCLUSIONS

A one-dimensional steady-state multiphysics model of a single VRFB, encompassing mass, charge, and momentum transport and conservation has been proposed. Compared to previous model in literature current collector have been included aiming at simulating real VRFB stacks. Comparisons with 2D steady-state multiphysics model show that the 1D assumption is reliable to properly simulate both electrical and chemical quantities. Starting from these models, reservoir equations and mass balance equations have been included in order to simulate charge-discharge operations and, in particular, to estimate the battery run-time.

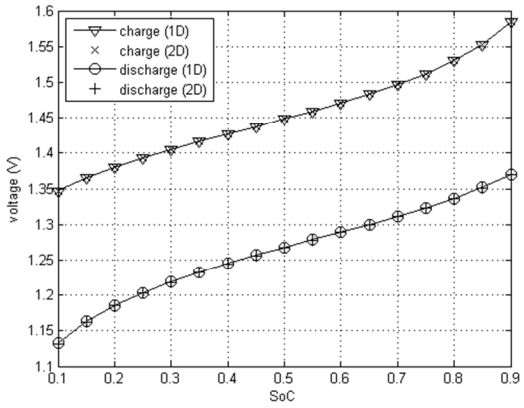

Figure 3: VRFB cell voltage vs. State of Charge.

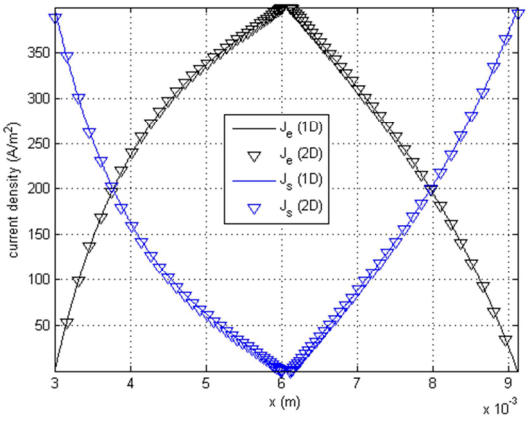

Figure 4: Electrolyte (J_e) and electrode (J_S) current density in electrode + membrane region.

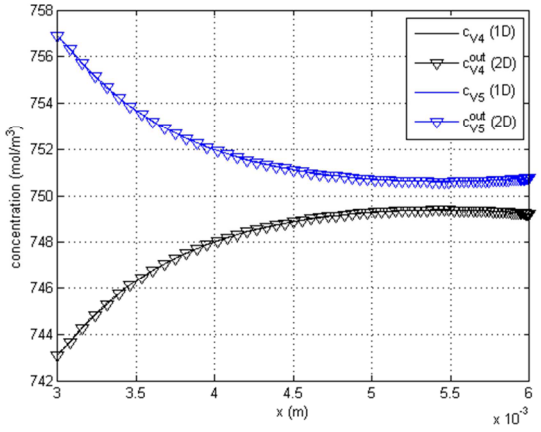

Figure 5: Positive electrode species concentrations c_{V4}, c_{V5} during charge phase ($SoC = 0.5$).

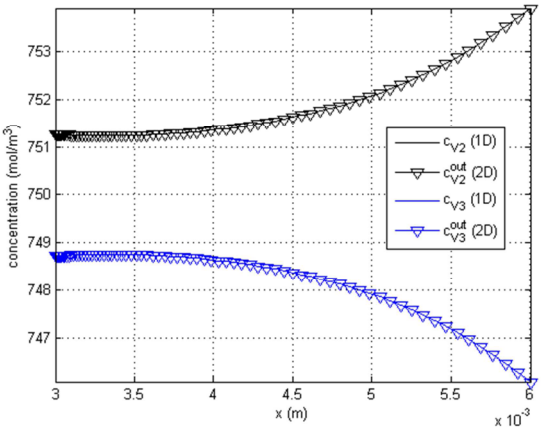

Figure 6: Negative electrode species concentrations c_{V2}, c_{V3} during charge phase ($SoC = 0.5$).

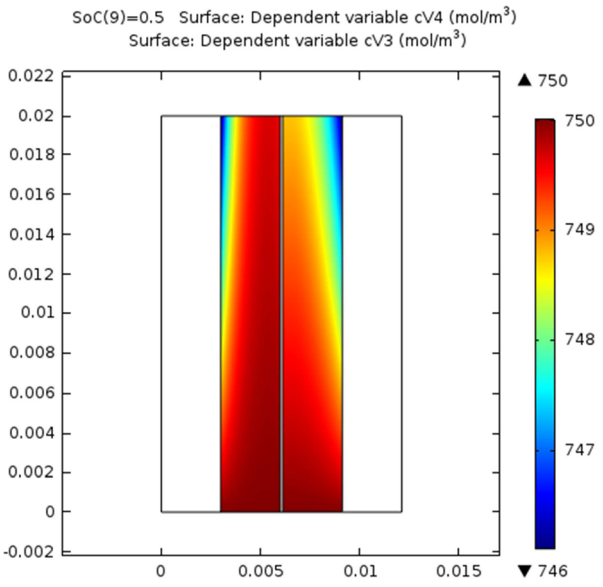

Figure 7: Reactant concentration c_{V4}, c_{V3} distributions during the charge phase (2D model, $SoC = 0.5$).

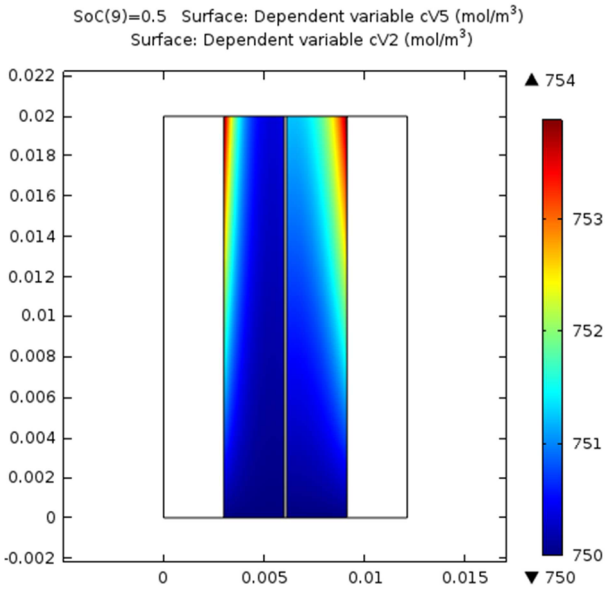

Figure 8: Product concentration c_{V5}, c_{V2} distributions during the charge phase (2D model, $SoC = 0.5$).

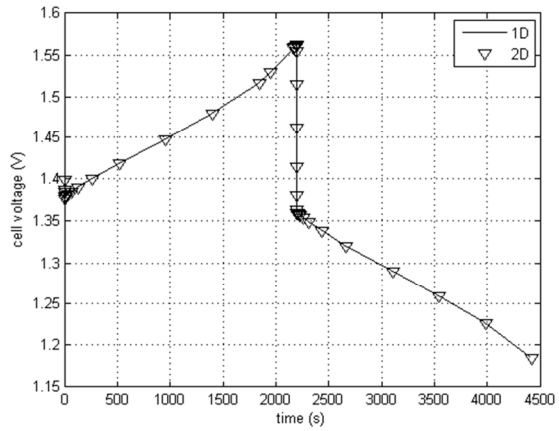

Figure 9: Cell voltage time profile during charge ($\Delta t_{ch} = 2200$ s) and discharge phases.

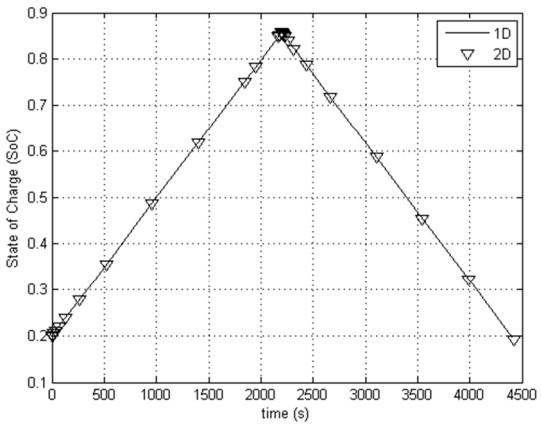

Figure 10: State of charge time profile during charge ($\Delta t_{ch} = 2200$ s) and discharge phases.

Table 1: Geometrical parameters of the 1D–2D VRFB model

h_m	$1.25 \cdot 10^{-4}$ m	PEM thickness
h_e	$3.00 \cdot 10^{-3}$ m	electrode thickness
h_c	$1.25 \cdot 10^{-4}$ m	collector thickness
L	$2.00 \cdot 10^{-2}$ m	cell length
w	$2.50 \cdot 10^{-2}$ m	cell width
V	$3 \cdot 10^{-6}$ m^3	reservoir volumes

Table 2: Physical parameters of the 1D–2D VRFB model

ϵ	0.929	electrode porosity
D_H	$9.3 \cdot 10^{-9}\epsilon^{1.5}$ m/s	H^+ diffusivity
D_{V4}	$3.9 \cdot 10^{-10}\epsilon^{1.5}$ m/s	V4 diffusivity
D_{V5}	$3.9 \cdot 10^{-10}\epsilon^{1.5}$ m/s	V5 diffusivity
D_{V2}	$2.4 \cdot 10^{-10}\epsilon^{1.5}$ m/s	V2 diffusivity
D_{V3}	$2.4 \cdot 10^{-10}\epsilon^{1.5}$ m/s	V3 diffusivity
D_{SO4}	$1.1 \cdot 10^{-9}\epsilon^{1.5}$ m/s	SO4 diffusivity
Q	60 ml/min	molar flow rate
v_y	$Q/h_e w\epsilon$	electrolyte velocity
T	300 K	cell temperature
σ_s	$1000 \cdot (1-\epsilon)^{1.5}$ S/m	solid phase conductivity
$E_{0,1}$	1.004 V	std potential (+)
$E_{0,2}$	-0.255 V	std potential (–)
K_1	$6.8{\cdot}10^{-7}$ m/s	rate constant (+)
K_2	$1.7{\cdot}10^{-7}$ m/s	rate constant (–)
A	$1.62{\cdot}10^4$ m^2/ m^3	specific area
α_1	0.5	transfer coefficient
α_2	0.5	transfer coefficient
J_{coll}	$\pm$ 400 A/m^2	collector current density (+: charge)
σ_c	1000 S/m	collector conductivity
$c_{V,1}$	1500 mol/m^3	tot concentration (+)
$c_{V,2}$	1500 mol/m^3	tot concentration (–)
$c^0_{H^+,1}$	6000 mol/m^3	H^+ concentration (+)
$c^0_{H^+,2}$	4500 mol/m^3	H^+ concentration (–)
c_f	1200 mol/m^3	fixed charge concentration (PEM)
$D_{H,m}$	$3.5 \cdot 10^{-10}$ m/s	H^+ diffusivity (PEM)
z_H	1	H^+ valence
z_{V2}	2	V2 valence
z_{V3}	3	V3 valence
z_{V4}	2	V4 valence
z_{V5}	1	V5 valence
$K_{m,1}$	$1.6 \cdot 10^{-4} ms^{-1}\left(v_y/1\,ms^{-1}\right)^{0.4}$	mass transfer coefficient (+)
$K_{m,2}$	$1.6 \cdot 10^{-4} ms^{-1}\left(v_y/1\,ms^{-1}\right)^{0.4}$	mass transfer coefficient (–)

REFERENCES

[1] Alotto, P., Guarnieri, M., and Moro, F., Redox flow batteries for the storage of renewable energy: A review, *Renewable and Sustainable Energy Reviews* (2014) **29**:325-335.
[2] Shah, A.A., Watt-Smith, A.A., and Walsh, F.C., A dynamic performance model for redox-flow batteries involving soluble species, *Electrochemica Acta* (2008) **53**:8087-8100.
[3] Knehr, K. W., et al., A Transient Vanadium Flow Battery Model Incorporating Vanadium Crossover and Water Transport Through the Membrane, *Journal of the Electrochemical Society* (2012) **159**:A1446-A1459.
[4] You, D., Zhang, H., and Chen, J., A simple model for the vanadium redox battery, *Electrochemica Acta* (2009) **54**:6827-6836.
[5] Chen, C.L., Yeoh, H. K., and Chakrabarti, M. H., An enhancement to Vynnycky's model for the all-vanadium redox flow battery, *Electrochemica Acta* (2014) **120**:167-179.